Effect of Stress Ratio(R) and Stress Concentration Factor (Kt) on Fatigue Properties of WSTi6211 Titanium Alloy

Hao Fang[1,2], Feng Yong[1,2], Du Yuxuan[1], Wang Yue[3], Xu Enen[2], Wang Kaixuan[2],Tian Yanwen[2]

[1]State Key Laboratory of Solidification Processing，Northwest Polytechnical University,Xi'an,Shaanxi 710072,China

[2] Western Superconducting Technologies Co., Ltd., Xi'an,Shaanxi 710018, China

[3] Xi'an University of Architecture and Technology，Xi'an,Shaanxi 710055, China

*Email: haofang85@163.com

Abstract: In this paper, the author studied the effects of different stress ratios（R） and stress concentration factors(K_t) on the fatigue properties of WSTi6211 titanium alloy.Through S-N curve, the author obtained the fatigue ultimate strength of the material under different conditions and analyzed characteristics of fatigue fractures, including the crack source, the crack growth region and the final rupture region. The results show that when K_t=1, R=0.5, the fatigue ultimate strength σ_D is 626MPa; when K_t=1, R=0.06, the fatigue ultimate strength σ_D is 527.5MPa; when K_t=3, R=0.06, the ultimate fatigue strength σ_D is 267MPa. Fatigue performance is very sensitive to R and K_t. The larger R is, the larger the fatigue ultimate strength is. The larger Kt is, the smaller the fatigue limit strength is. The fracture morphology shows typical fatigue fracture morphology. Most of the cracks originate on the surface of specimens and have typical fatigue bands. With the decrease of stress, the area of crack growth zone increases.

Key words: WSTi6211 Titanium Alloy; S-N Curve; Stress Ratio; Stress Concentration Factor

1.Intrpduction

"A generation of materials, a generation of equipment".[1] Titanium alloy is an advanced aviation material with a density of only 4.5g/cm^3. It has excellent corrosion resistance, higher specific strength, good high temperature performance and fatigue resistance, and has become one of the main structural materials of modern aircraft. At present, the use of titanium alloys in aircraft has become one of the important indicators to measure its advancement. For example, the use of titanium alloys in F-22 of the fourth generation aircraft in the United States has reached 41%. With the development of aviation technology, the requirement of combat performance, maneuverability, reliability and service life of aircraft has been improved, and the amount of high-end titanium alloys used in new aircraft will continue to increase.

WSTi6211, similar to TA15 titanium alloy, is a near-alpha titanium alloy with high $[Al]_{eq}$. It has medium room temperature and high temperature strength, good thermal stability and weldability. It is an important titanium alloy material for aircraft and can be used for a long time from 450℃ to 500℃[2]. Fatigue property of materials is usurally an important factor that directly affects their service life. There are many reports on the study of microstructure, fatigue properties and fracture behavior of titanium alloys. However, most literatures focus on the comparison of fatigue deformation characteristics between lamellar structure obtained by single-phase deformation and bimodal structure obtained by two-phase deformation[3-8]. However, the effect of R and K_t on the equiaxed structure of the alloy has rarely been reported. In this paper, the effects of Kt and R on fatigue properties were studied, and the fracture morphology characteristics were analyzed, which lays a theoretical foundation for exploiting the potential application of materials.

2. Material and experiments

2.1 Experimental Materials

The experimental material is WSTi6211 titanium alloy bar with 300mm diameter. The chemical composition is shown in Table 1. The phase transformation temperature is 995 ± 5 ℃. The heat treatment mode is 840 C/2.5h, AC.

Table 1 The composition of WSTi6211

s	Al	Mo	V	Zr	Si	O	Ti
Wt.%	6.89	1.77	2.33	2.32	0.024	0.12	Bal.

The microstructure of WSTi6211 titanium alloy bar is typical equiaxed structures processed in two-phase zone. The content of α phase is about 70% and the size is about 10-20μm. Shown in Fig.1.

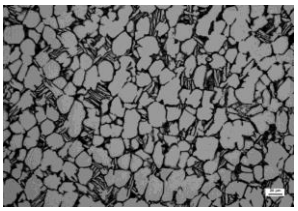

Fig.1 Microstructure of WSTi6211

1.2 Experimental Method

High cycle fatigue test was carried out on Zwick Amsler HFP 5100 high frequency fatigue testing machine. The frequency f is 120 Hz, stress amplitude control with sine wave. When the minimum number of cycles is exceeds 1.0×107 times, if the sample is not broken, the test will be terminated artificially and the sample passed the test.

The testing process conforms to GB/T3075-2008 with atmospheric environment and RT. The high cycle fatigue properties of the alloy were tested by group method and lifting method, and the S-N curve was drawn. The conditional fatigue ultimate strength of the alloy was determined by lifting method formula. The sample size is shown in Fig.2.

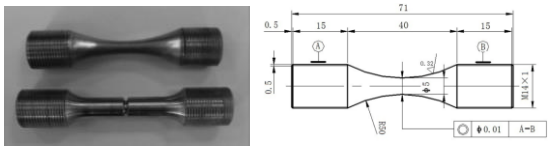

Fig.2 Size of sample

According to the design parameters of the alloy used in aeronautical structures, three groups of typical tests were designed in this experiment.

(1)Kt=1,R=0.06;

(2)Kt=1,R=0.5;

(3)Kt=3,R=0.06.

1.3 Fracture Morphology Observation

After the fatigue loading test, the fracture morphology of specimens under different loading conditions was observed by JSM4640 SEM. The characteristics of fatigue crack source, propagation zone and instantaneous fracture zone from high stress zone to low stress zone were observed. The sensitivity of the alloy to stress ratio and stress concentration factor was analyzed.

3 Results

3.1 Fatigue Performance of K_t=1,R=0.5

Under the test conditions of K_t=1 and R=0.5, the median fatigue life corresponding to the maximum stresses of 1000 MPa, 900 MPa and 800 MPa is 6.8×10^4、2.58×10^5 and 1.108×10^6 respectively. The fatigue ultimate strength was measured by lifting method. As shown in Table 2 and Fig.3, the maximum stress ranged from 600 MPa to 660 MPa, which consisted of five pairs. The fatigue ultimate strength σ_D=626MPa and the C_v was 0.0313.

Table 2 Fatigue Performance (K_t=1,R=0.5)

Group experiment					
Sample No.	σ_{max}（MPa）	N cycle	N_{50}cycle	C_V	Notes
22	1000	6.9×10^4	6.8×10^4	0.025	/
6	1000	8.0×10^4			/
3	1000	7.8×10^4			/
24	1000	4.4×10^4			/
9	900	2.54×10^5	2.58×10^5	0.007	/
18	900	2.33×10^5			/
16	900	2.88×10^5			/
15	900	2.59×10^5			/
25	800	1.336×10^6	1.018×10^6	0.0232	/
21	800	1.067×10^6			/
10	800	1.042×10^6			/
17	800	6.27×10^5			/
11	720	2.190×10^6	/	/	Invalid

Lifting method experiment			
Sample No.	σ_{max}（MPa）	N cycle	Notes
14	660	3.125×10^6	/
8	640	6.575×10^6	/
20	640	5.873×10^6	/
4	640	$>1.0000\times10^7$	/
2	620	5.379×10^6	/
7	620	4.425×10^6	/
13	620	$>1.0000\times10^7$	/
12	620	$>1.0000\times10^7$	/
19	620	$>1.0000\times10^7$	Invalid
23	600	$>1.0000\times10^7$	/
5	600	$>1.0000\times10^7$	/

σ_D（MPa）	C_V	Notes
626	0.0313	5 paires

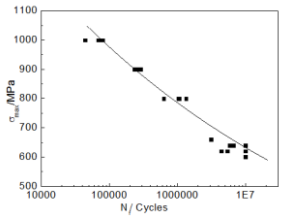

Fig 3 S-N curve（K_t=1,R=0.5）

3.2 Fatigue Performance of K_t=1,R=0.06

Under the test conditions of K_t=1 and R=0.06, the median fatigue life corresponding to the maximum stresses of 900 MPa, 800 MPa and 700 MPa is 3.4×10^4、1.40×10^5 and 6.80×10^6 respectively. The fatigue ultimate strength was measured by lifting method. As shown in Table 3 and Fig.4, the maximum stress ranged from 500 MPa to 550 MPa, which consisted of five pairs. The fatigue ultimate strength σ_D=527.5MPa and the Cv was 0.026.

Table 3 Fatigue Performance (K_t=1,R=0.06)

Group experiment					
Sample No.	σ_{max}	N	N_{50}cycle	C_V	Notes
47	900	2.7×10^4	3.4×10^4	0.0161	/
35	900	3.3×10^4			/
49	900	3.8×10^4			/
46	900	3.9×10^4			/
39	800	7.1×10^4	1.40×10^5	0.0476	/
28	800	8.7×10^4			/
33	800	1.69×10^5			/
45	800	2.34×10^5			/
40	700	3.09×10^5	6.80×10^5	0.0498	/
48	700	3.56×10^5			/
41	700	8.67×10^5			/
31	700	1.187×10^6			/
42	600	1.522×10^6	/	/	Invalid
27	600	3.047×10^6	/	/	Invalid
Lifting method experiment					
Sample No.	σ_{max}	N			Notes
37	550	5.198×10^6			/
32	550	7.887×10^6			/
30	550	8.128×10^6			/
34	525	1.915×10^6			/
44	525	3.148×10^6			/
43	525	$>1.0000\times10^7$			/
38	525	$>1.0000\times10^7$			/
50	525	$>1.0000\times10^7$			/
29	500	$>1.0000\times10^7$			/
36	500	$>1.0000\times10^7$			/
σ_D（MPa）		C_V			Notes
527.5		0.026			5 paires

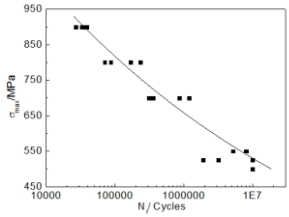

Fig 4 S-N curve（K_t=1,R=0.06）

3.3 Fatigue Performance of K_t=3,R=0.06

Under the test conditions of K_t=3 and R=0.06, the median fatigue life corresponding to the maximum stresses of 400MPa, 350MPa and 300MPa is 1.13×10^5、5.79×10^5 and 1.772×10^6 respectively. The fatigue ultimate strength was measured by lifting method. As shown in Table 4 and Fig 5, the maximum stress ranged from 250 MPa to 280 MPa, which consisted of five pairs. The fatigue ultimate strength σ_D=267MPa and the Cv was 0.0313.

Table 2 Fatigue Performance (K_t=3,R=0.06)

Group experiment					
Sample No.	σ_{max}	N	N_{50}cycle	C_V	Notes
3	400	4.5×10^4	1.13×10^5	0.0791	/
6	400	3.5×10^4			/
17	400	2.10×10^5			/
21	400	1.61×10^5			/
7	350	5.7×10^4	5.19×10^5	0.1023	/
4	350	2.95×10^5			/
22	350	4.26×10^5			/
5	350	1.297×10^6			/
8	300	3.62×10^5	1.772×10^6	0.0655	/
24	300	1.830×10^6			/
13	300	1.902×10^6			/
14	300	2.996×10^6			/
Lifting method experiment					
Sample No.	σ_{max}	N			Notes
1	280	1.170×10^6			/
2	280	4.607×10^6			/
15	270	4.316×10^6			Invalid
23	270	2.037×10^6			/
11	270	3.087×10^6			/
25	270	$>1.0000\times10^7$			/
19	270	$>1.0000\times10^7$			/
18	260	8.847×10^6			/
9	260	$>1.0000\times10^7$			/
12	260	$>1.0000\times10^7$			/
20	250	$>1.0000\times10^7$			/
σ_D（MPa）		C_V			Notes
267		0.0313			5 paires

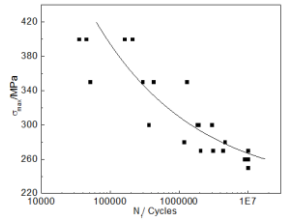

Fig 5 S-N curve（K_t=3,R=0.06）

4 Discussion

4.1 Effect of R on Fatigue Properties

Comparing to the fatigue properties of the material under different R conditions, it can be seen that when the maximum stress is 900MPa, the fatigue life of the material is 2.58×10^5 under condition of R=0.5 and which is 3.4×10^4 when the stress ratio R=0.06.When the maximum stress is 800 MPa, the fatigue life is 1.108×10^6 when R=0.5 and 1.4×10^5 when R=0.06. At the same time, the fatigue ultimate strength also decreased from 626 MPa to 527.5 MPa. The fatigue limit of materials reflects the comprehensive ability of materials to resist crack initiation and propagation. Which shows that the greater the stress ratio, the greater the fatigue life of the material, and the greater the impact on the fatigue ultimate strength.

4.2 Effect of K_t on Fatigue Properties

Comparing to the fatigue properties of the material under different K_t conditions, it can be seen that when K_t=3, σ_D is 267 MPa, which is about 1/2 of the value when K_t=1. The fatigue property of the material is greatly affected by Kt. When the specimen is changed from smooth to notched, the fatigue limit loss of the material is

very large.

4.3 High cycle fatigue fracture characteristics

The fracture characteristics of fatigue fracture are analyzed. The macro fracture morphology is divided into three distinct regions, including the crack source, the crack growth regione and the final rupture region In this experiment, when K_t=1, both in high and low stress regions, cracks begin to initiate and propagate on the surface, and the location of the initiation is relatively clear. When K_t=3, there are multiple fatigue crack initiation points. Radial river patterns can be clearly seen near the germination point.

The fatigue band is a groove pattern which is slightly curved and parallel to each other. It is perpendicular to the direction of crack propagation. It is the microcosmic trace left by crack propagation and the most typical microcosmic feature of fatigue fracture. There are obvious fatigue bands in the crack propagation zone. The fatigue bands are fine under low stress. Grain boundary plays an important role in the fatigue crack propagation. The crack front is blocked near the grain boundary, and the striation direction changes when the crack transits from one grain to the adjacent one. Under high stress, the crack propagation is faster, the fatigue strip bandwidth is wider, and the crystallographic characteristics of the stripe are not obvious[6].

In the high stress region (σ_{max}=900MPa), near the fatigue source region, the fracture morphology has slip steps and cleavage characteristics, and the cyclic loading times are few, and the fatigue band characteristics are not obvious，shown in Fig.6. In the medium stress region (σ_{max}=600MPa), the crack growth area is large and the fatigue band characteristics are obvious, shown in Fig.7. In the low stress region (σ_{max}=300 MPa), the crack initiation point increases and the fatigue band characteristics are obvious, shown in Fig.8. The instantaneous fracture zone, i.e. the area formed by the unstable propagation of the crack, presents dimples, which belongs to the typical ductile fracture characteristics. As the stress decreases, the area of fatigue crack growth zone increases.

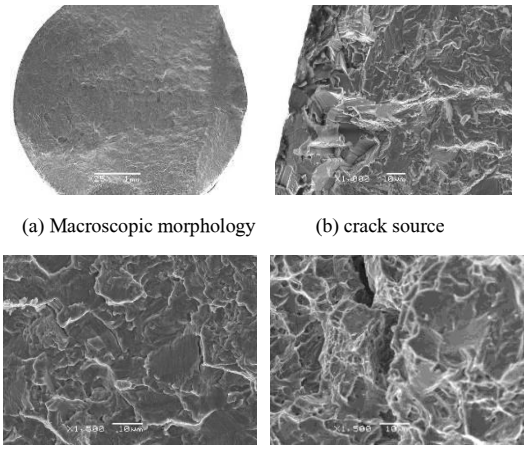

(a) Macroscopic morphology (b) crack source

(c) crack growth region (d) final rupture region

Fig.6 Fracture morphology（Kt=1,R=0.06， σ_{max}=900MPa）

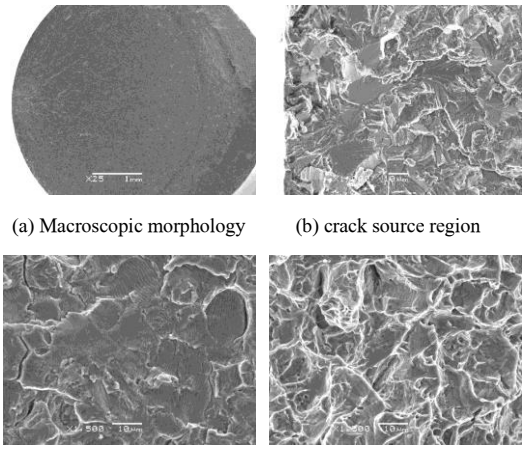

(a) Macroscopic morphology (b) crack source region

(c) crack growth region (d) final rupture region

Fig.7 Fracture morphology（Kt=1,R=0.06， σ_{max}=600MPa）

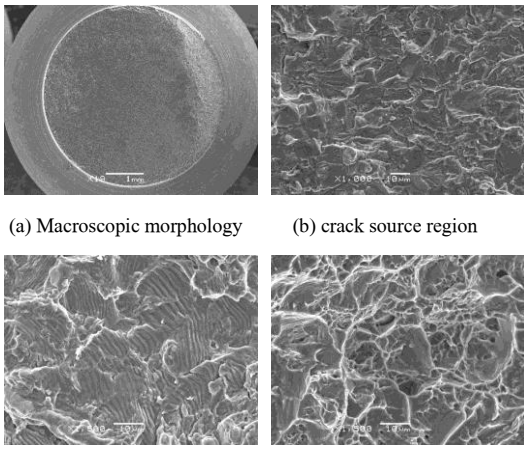

(a) Macroscopic morphology (b) crack source region

(c) crack growth region (d) final rupture region

Fig.8 Fracture morphology（Kt=3,R=0.06， σ_{max}=300MPa）

5 Conclusion

(1) R has a great influence on the fatigue properties of WSTi6211 titanium alloy. With the increase of R, the_D of the material increases. When R increases from 0.06 to 0.5, the corresponding_D increases from 527.5 MPa to 626 MPa.

(2) Kt has a great influence on fatigue properties of WSTi6211 titanium alloy. When Kt increases from 1 to 3, the corresponding_D decreases from 527.5 MPa to about 50%.

(3) The fracture morphology shows typical fatigue fracture morphology. The crack initiation point is more than the sample surface, and there are typical fatigue bands. With the decrease of stress, the area of crack propagation area increases.

6 Acknowledgements

Thank my tuter, classmates and colleagues and they gave me lots help during experiments.

7 Reference:

[1] Cao Chunxiao. Generation Material Technology, Generation Large Aircraft [J]. Acta Aeronautica ET Astronautica Sinica. 2008, 29(3): 701-706.

[2]Li Xingwu,Liu Ruiming,Sha Aixue,Chu Junpeng etc. EFFECT OF MICROSTRUCTURE ON FATIGUE PROPERTIES OF TA15 ALLOY [J]. Acta Metallurgica Sinica, 2002, 38(supplementary issue):280-281.

[3]CAO Jing-xia,HUANG Xu, LI Zhen-xi，High Cycle Fatigue Properties and Fracture Features of TA15 Titanium Alloy[J]，Journal of Materials Engineering，2004.3（3）：28-34

[4]J A Hines,G lutjering. Propagation of microcracks at stress amplitudes below the convertional fatigue limit in Ti-6Al-4V[J].Fatigue Fract Eng Mater Sruct,1999,22(8):657-666

[5]A L Dowson,C J Beevers and L Grabowski.The Microstructual Features Associated with the Growth of Short Fatigue Cracks in a Near-Alpha Ti Alloy[A].F H Fores and I Caplan.Titanium Science and Technology[C].TMS.1993.1741-1748

[6]G Lutjering.Influence of Processing on Microstructure and Mechanical Properties of (α + β) Titanium Alloys[J].Mat Sci Eng,1998.A243:32-45.

[7] W J Evans.Optimising Mechenical Properties in Alpha+Beta Titanium Alloys[J]. Mat Sci Eng,1998,A243:89-96.

[8] M Ya Brun，G V Shakhanova,Titanium Alloy Structure and Pramaters Defining Its Diversity[J],Titanium Science Technical Journal,1993,1（3）：24-29

.